

Chapter 13

Modeling of Atmospheric Mercury Deposition in India



Krish Vijayaraghavan, Shari Libicki, Ross Beardsley, and Sunil Ojha

13.1 Introduction

Mercury (Hg) is a hazardous pollutant that could affect human health and ecosystems. Human exposure to elemental mercury vapours is a health concern at very high concentrations because of toxic inhalation (Clarkson et al. 2003). In addition, inorganic Hg emitted to the atmosphere will ultimately deposit to the surface of the earth where it can be transformed to the more harmful form, methylmercury, that can bioaccumulate in fish and other food chains (Schroeder and Munthe 1998; Seigneur et al. 2001; Pirrone and Mahaffey 2005). While developing fetuses are particularly vulnerable because of its neurotoxicity, there are also concerns due to health effects on sensitive humans and wildlife (Driscoll et al. 2013).

Atmospheric inorganic Hg exists in three forms: (1) elemental mercury vapour, Hg^0 , also referred to as gaseous elemental mercury (GEM), (2) gaseous divalent mercury, Hg^{II} , also known as gaseous oxidized mercury (GOM), and (3) particulate mercury, Hg_p , also referred to as particle bound mercury (PBM). Hg_p can arise from GOM becoming adsorbed to atmospheric particulate matter after it is emitted in vapour form or from divalent Hg being emitted into the atmosphere as particulate matter directly in the flue gas. These three forms of Hg vary in their physical and chemical properties and, therefore, have different deposition rates and atmospheric lifetimes. Because Hg^0 has low reactivity and solubility (e.g., Lindberg et al. 2007), it has a lifetime of several months to a year and may be transported across continents. In contrast, Hg^{II} and Hg_p have lifetimes ranging from hours to days because they have

K. Vijayaraghavan (✉) · S. Libicki · R. Beardsley
Ramboll, Novato and San Francisco, CA 94945, USA
e-mail: kvijayaraghavan@ramboll.com

S. Ojha
Ramboll India, Gurgaon 122002, India
e-mail: suojh@ramboll.com

high wet and dry deposition rates near their sources. The different forms of Hg also inter-convert between each other through gas- and aqueous-phase chemical reactions (e.g., Schroeder and Munthe 1998; Lin et al. 2006; Seigneur et al. 2006) which affects their lifetimes. Due to the long-range transport of Hg, recovery of ecosystems influenced by atmospheric deposition would be influenced both by reductions in local emissions as well as changes in global Hg emissions (e.g., Vijayaraghavan et al. 2014).

Emission inventories have been compiled in numerous studies for large sources in India including coal-based thermal power plants, waste incineration, ferrous and non-ferrous metal production, cement production and the chlor-alkali industry (Mukherjee et al. 2009; Streets et al. 2009; Pirrone et al. 2010; Sloss 2012; AMAP/UNEP 2013; Chakraborty et al. 2013; Rai et al. 2013). Examining the extent of Hg deposition in India allows us to understand the potential contributions of Hg air emissions in the country as well as upwind sources to deposition in the region.

In this paper, an overview of the atmospheric Hg model and application for this study is first presented. The emissions' inventory utilized is discussed, followed by a description of other model inputs and the model configuration. Results are presented for Hg wet and dry deposition across India in general and in specific areas. Major sources of uncertainties in the modeling study are discussed.

13.2 Modeling Methodology

Due to the potential for Hg to undergo long-range transport, it is essential to use a modeling approach that takes into account the global cycling of Hg. In this study, we apply the Goddard Earth Observing System Chemistry (GEOS-Chem) model (www.geos-chem.org), a global three-dimensional (3D) chemistry transport model that uses meteorology from the Goddard Earth Observing System (GEOS) of the National Aeronautics and Space Administration (NASA) Global Modeling and Assimilation Office (GMAO). GEOS-Chem was first developed by the Atmospheric Chemistry Modeling Group (ACMG) at Harvard University over fifteen years ago (Bey et al. 2001) and adapted for Hg cycling by Selin et al. (2007) and Strode et al. (2007). It dynamically couples a 3D atmosphere (Selin et al. 2007), a 2D terrestrial reservoir (Selin et al. 2008) and a 2D ocean module (Soerensen et al. 201). The model has since been extensively evaluated for air concentrations and/or wet deposition in several other global Hg deposition studies (e.g., Holmes et al. 2010; Corbitt et al. 2011; Amos et al. 2012; Chen et al. 2014; Song et al. 2015; Zhang et al. 2016).

We applied version 10-01 of GEOS-Chem using a modeling grid over the entire world with a horizontal grid resolution of 2 by 2.5° (latitude and longitude, respectively). The model simulates the emissions, dispersion, conversion, and wet and dry deposition of Hg⁰, Hg^{II} and Hg_p in the atmosphere. An annual simulation was conducted for 2011 using year 2010 for model initialization (spin-up). Assimilated vertical and surface meteorological data were obtained from the NASA GMAO GEOS-5 data for 2011 and used for the modeling. Mercury deposition fluxes over

India, and parts of neighbouring countries were extracted from this GEOS-Chem global simulation output.

The model includes the gas-phase oxidation of Hg^0 to Hg^{II} by bromine and the aqueous-phase photoreduction of Hg^{II} to Hg^0 (Holmes et al. 2010). The dry deposition algorithm is from Wesely (1989) and is based on a resistances-in-series method. Hg^0 evasion includes volatilization from soil and rapid recycling (re-emission) of newly deposited Hg (Selin et al. 2008; Wang et al. 2016). The former is estimated as a function of soil Hg content and solar radiation. The latter is modeled by recycling a fraction of deposited Hg^{II} to the atmosphere as Hg^0 immediately after deposition. Wet deposition follows scavenging of Hg^{II} and Hg_p which is based on Liu et al. (2001). Below-cloud scavenging of Hg_p by snow is also included (Holmes et al. 2010; Amos et al. 2012; Zhang et al. 2012). The wet deposition of Hg^0 is negligible because it is sparingly soluble in water.

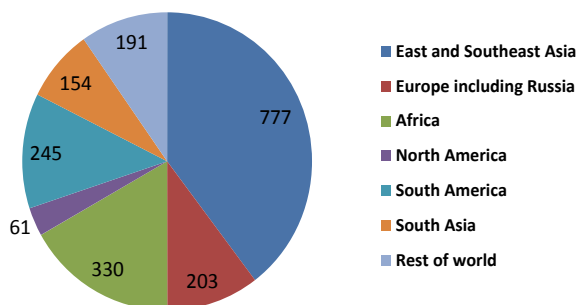
Worldwide Hg emissions from the following source categories are included in the modeling: (1) Anthropogenic emissions of Hg^0 , Hg^{II} and Hg_p , (2) Hg^0 emissions from biomass burning, (3) Hg^0 emissions from land (including re-emissions of previously deposited Hg) and (4) Hg^0 emissions from oceans (including re-emissions).

13.2.1 Mercury Emissions

The anthropogenic emissions used in the modeling is based on the 2010 global Hg inventory from the Arctic Monitoring and Assessment Programme (AMAP)/United Nations Environment Programme (UNEP) 2013 global mercury assessment (AMAP/UNEP 2013, 2015).

The total estimated worldwide anthropogenic Hg emission in 2010 is $1960 \text{ Mg year}^{-1}$ (AMAP/UNEP 2013). Fossil fuel (mainly coal) combustion for power and heating is the largest single category of emissions from anthropogenic sources. Other important source categories are artisanal and small-scale gold production (mainly in Asia and South America), cement production and metal production (mainly in Asia) and waste incineration. Figure 13.1 (adapted from data in AMAP/UNEP 2013) shows the contributions of different source regions to global

Fig. 13.1 2010 global anthropogenic mercury emissions inventory used in modeling (Mg year^{-1}). Source AMAP/UNEP (2013)



anthropogenic Hg emissions in 2010. East and Southeast Asia together constitute the largest contributor at 40% of the total (with the majority from China at 575 Mg year^{-1}), followed by Africa, South America and Europe. The total estimated anthropogenic Hg emission from South Asia (consisting of Afghanistan, Bangladesh, Bhutan, India, Maldives, Nepal, Pakistan and Sri Lanka) is 154 Mg year^{-1} , representing 8% of the worldwide anthropogenic inventory. Coal combustion and cement production are estimated to contribute 59% and 11%, respectively, to the South Asian total.

Large uncertainties exist, in general, in modeled global mass balances of Hg and, in particular, in air emission inventories due to variability in input parameters and process rates (e.g., Qureshi et al. 2011). The values reported above are best estimate values from the AMAP/UNEP inventory, with a range of $1010\text{--}4070 \text{ Mg year}^{-1}$ for the global Hg emission total.

Table 13.1 shows estimated Hg emissions from India in 2010 from the AMAP/UNEP (2013) inventory as applied in the current study. The total estimated anthropogenic Hg emission from India is 145 Mg year^{-1} with the uncertainty ranging from 75 to 330 Mg year^{-1} . Emissions from coal combustion dominate the inventory with coal burning in power plants, industrial uses and domestic/residential use constituting 62% (or 90 Mg year^{-1}) of the total Hg emissions. Waste disposal and cement production constitute approximately 9% each, while copper and zinc production each represent approximately 7.5%.

Total coal consumption at 111 coal-burning thermal power plants in India during the 2010–2011 period was an estimated 500 million Mg year^{-1} (Guttikunda and Jawahar 2014). Rai et al. (2013) estimated uncontrolled Hg emissions from combustion of coal in India in 2010–11 to be 160 Mg year^{-1} based on total coal consumption of a similar amount ($590 \text{ million Mg year}^{-1}$) and an average Hg content in coal of 0.272 ppm. The estimated emissions rate would be lower when considering particulate control devices in place. Historic estimates of Hg emissions in India are generally higher. For example, Mukherjee et al. (2009) estimated that 2004 Hg emissions in India were $222\text{--}310 \text{ Mg year}^{-1}$. Sloss (2012) summarized the Indian anthropogenic Hg emissions inventory from the prior 2008 AMAP/UNEP assessment that used a 2005-year datum. Emissions of Hg in India were estimated to be 161 Mg year^{-1} in 2005. However, a direct comparison between the 2005 and 2010 AMAP inventories is not possible because of changes in the methodology between the two assessments (AMAP/UNEP 2013).

Chakraborty et al. (2013) quantified anthropogenic Hg flows in India; air emissions were estimated to be 235 Mg year^{-1} in 2010. This value is at the higher end of the AMAP/UNEP range and higher than the value (145 Mg year^{-1}) in the current study. Differences are likely due to difference in methodology and activity data between the two studies. However, the fraction of the total due to coal combustion is comparable between the two inventories, at approximately 60%.

Hg emissions from biomass burning are based on version 3 of the Global Fire Emission Database (van der Werf et al. 2010) for carbon monoxide (CO) and a Hg:CO ratio of $100 \text{ nmol mol}^{-1}$ (Holmes et al. 2010; Song et al. 2015). This results in a global total biomass burning emission of 210 Mg year^{-1} . The

Table 13.1 Estimated 2010 anthropogenic Hg emissions from India used in modeling (kg year^{-1})

Source category	Hg emissions (kg year^{-1})
Bituminous coal combustion in power plants	41,387.5
Hard coal (bituminous/antracite) combustion in industrial use	22,677.2
Coal combustion for domestic/residential use, transport, etc.	16,033.7
Waste and other losses due to breakage and disposal in landfill, etc.	13,691.8
Cement production	13,420.8
Non-ferrous metal production: copper	10,939.6
Non-ferrous metal production: Zn	10,809.8
Lignite coal combustion in power plants	8056.3
Production of iron and steel	1934.3
Brown coal/lignite combustion in industrial use	1289.8
Artisanal and small-scale gold mining	1125.0
Caustic soda production	940.0
Oil refining	634.3
Human cremation (dental amalgams)	607.7
Non-ferrous metal production: Aluminium	464.0
Non-ferrous metal production: Lead	168.6
Non-ferrous metal production: gold large-scale	154.0
Heavy fuel oil combustion in industrial use	136.2
Light fuel oil combustion for domestic/residential use, transport	71.4
Heavy fuel oil combustion for domestic/residential use, transport	64.1
Waste incineration	42.5
Light fuel oil combustion ind. use	30.6
Heavy fuel oil combustion in power plants	28.9
Light fuel oil combustion in power plants	16.5
Natural gas combustion in power plants	6.4
Natural gas combustion in industrial use	1.5
Natural gas combustion for domestic/resident. Use, transport	0.5
Total	144,733

Source AMAP/UNEP (2013)

other non-anthropogenic Hg emission categories (Song et al. 2015) include land geogenic emissions (90 Mg year^{-1}), soil emissions parameterized as a function of solar radiation ($1680 \text{ Mg year}^{-1}$), re-emissions from soil, vegetation and snow-pack (520 Mg year^{-1}), and net ocean emissions ($3000 \text{ Mg year}^{-1}$). Thus, the total modeled worldwide mercury emission from biomass burning and natural sources is approximately $5500 \text{ Mg year}^{-1}$.

Figure 13.2 shows the spatial distribution of modeled anthropogenic Hg emissions in India and surrounding regions. Anthropogenic emissions are highest in the region

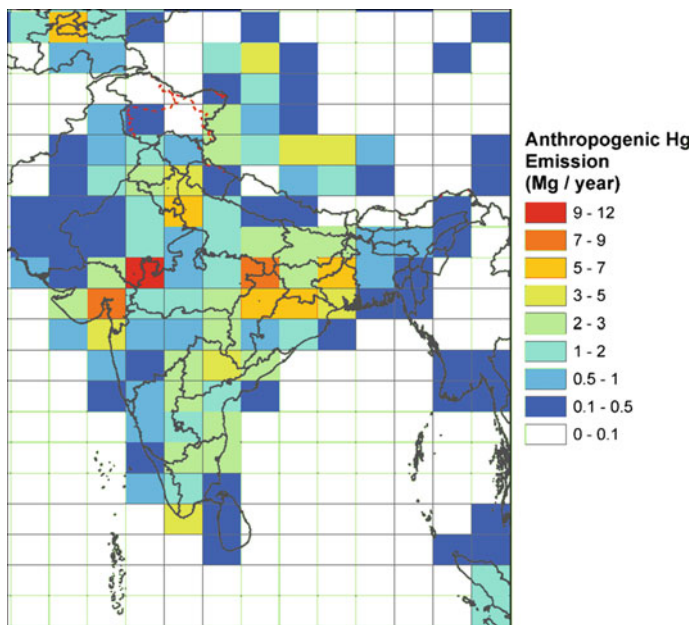


Fig. 13.2 Anthropogenic mercury emissions in the modeling grid in India and surrounding regions

near the southeastern part of the state of Rajasthan and the westernmost part of the state of Madhya Pradesh (MP) due to a combination of coal-based thermal power plants and non-ferrous metal (zinc and copper) production in the region. Hg emissions are also very high in the area encompassing eastern MP and southeastern part of the state of Uttar Pradesh (UP) and central/northern Chhattisgarh; this region has some of the highest density of coal-fired thermal power plants in the country due to proximity to coal mines.

The natural emissions and re-emissions of Hg are mainly from evasion from land (soil/vegetation emissions and re-emissions) with a total across India of 75 Mg year^{-1} (Fig. 13.3). Thus, when combined with the anthropogenic inventory of 145 Mg year^{-1} , the total annual Hg emission from India is estimated to be 220 Mg year^{-1} (Fig. 13.4).

13.3 Results and Conclusions

Figure 13.5 depicts the worldwide annual total (i.e., sum of wet and dry) deposition flux of Hg. Deposition shown is for total Hg, i.e., the sum of Hg^0 , Hg^{II} and Hg_p . The annual Hg deposition flux ranges from 0 to $125 \mu\text{g m}^{-2} \text{ year}^{-1}$ across the world, with high deposition (values exceeding $50 \mu\text{g m}^{-2} \text{ year}^{-1}$) over polluted regions including East and South Asia, western Europe, parts of Africa and South

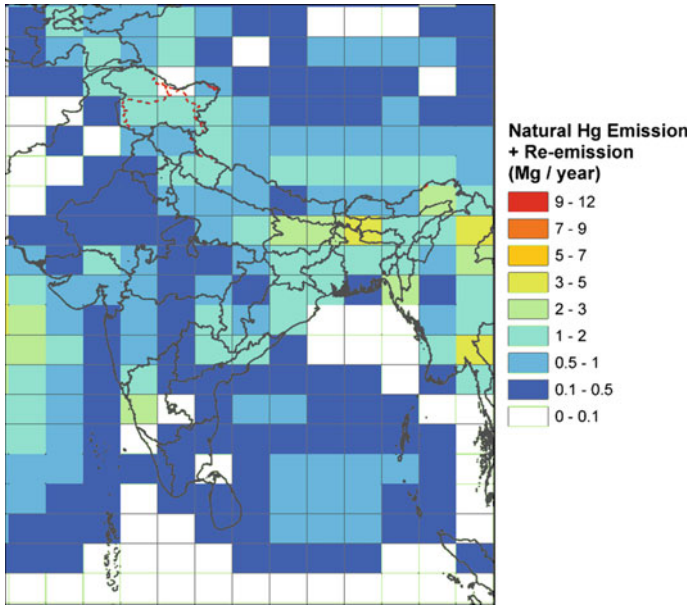


Fig. 13.3 Annual natural mercury emissions plus re-emissions in the modeling grid in India and surrounding regions

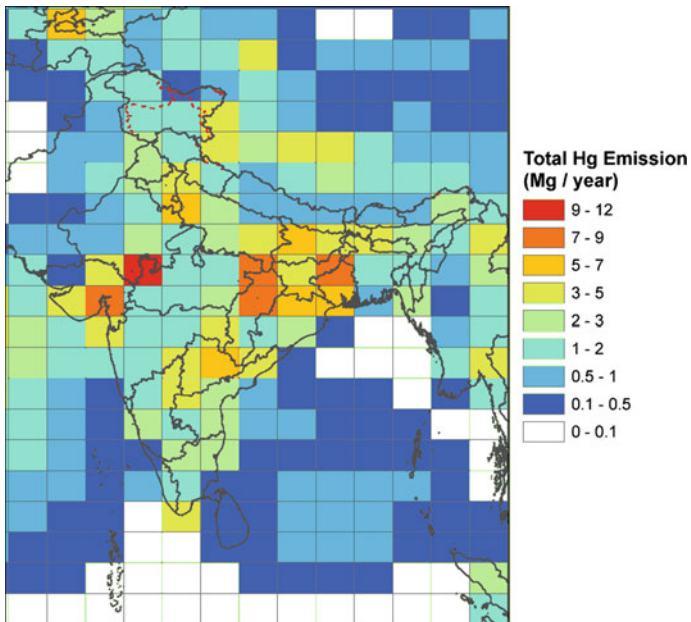


Fig. 13.4 Annual total (anthropogenic + natural + re-emitted) mercury emissions in the modeling grid in India and surrounding regions

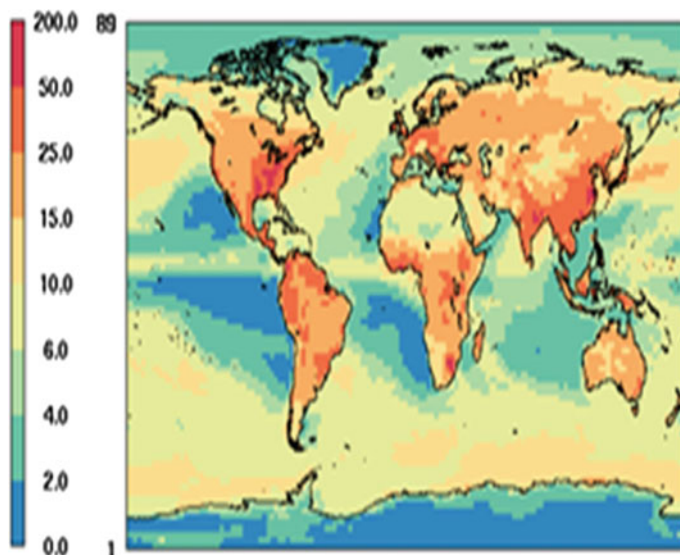


Fig. 13.5 Annual total deposition flux of total mercury ($\mu\text{g m}^{-2} \text{year}^{-1}$)

America, and the eastern United States. In addition to deposition in industrial regions due to local anthropogenic sources, the global deposition pattern also reflects the oxidation of Hg^0 and subsequent deposition as well as the air-surface exchange of Hg^0 associated with vegetated surfaces and high precipitation over some remote areas (AMAP/UNEP 2013).

The annual Hg deposition flux over the Indian mainland ranges from 10 to $57 \mu\text{g m}^{-2} \text{year}^{-1}$ (Fig. 13.6) with over four-fifths of the land area with deposition exceeding $25 \mu\text{g m}^{-2} \text{year}^{-1}$. In particular, the highest Hg deposition is seen in northern Chhattisgarh, eastern MP, Jharkhand and West Bengal, all regions with high Hg emissions. The annual deposition in those regions ranges from 50 to $57 \mu\text{g m}^{-2} \text{year}^{-1}$. These estimates are comparable to the peak deposition fluxes of 49 to $61 \mu\text{g m}^{-2} \text{year}^{-1}$ over south Asia reported by Giang et al. (2015) who modeled Hg deposition with GEOS-Chem v. 9-02 using a 2006 global Hg inventory.

The average annual Hg deposition flux over India in the current study is $27.6 \mu\text{g m}^{-2} \text{year}^{-1}$, resulting in a total Hg deposition to land over India of approximately 82Mg year^{-1} . This estimate is approximately 44% higher than the 57Mg year^{-1} total estimated by Qureshi (2016) using a Hg cycling box model. Deposition over India is due to both emissions within the country and long-range Hg transport from upwind sources. The modeled deposition over India is less than 40% of the total estimated emissions of 220Mg year^{-1} , suggesting that a large fraction of Indian Hg emissions is exported outside the country via atmospheric transport. No separate modeling was performed here to quantify upwind source contributions.

The modeled wet deposition (Fig. 13.7) is due to a combination of precipitation and Hg emissions. The annual wet deposition flux over the Indian mainland

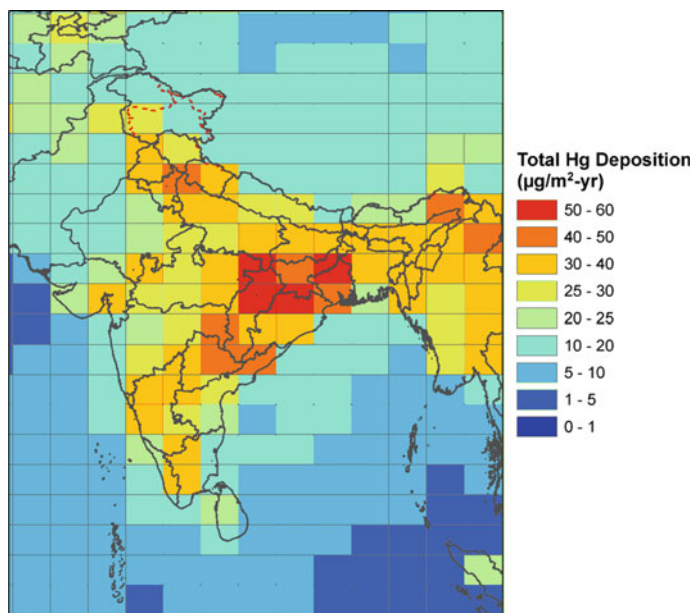


Fig. 13.6 Annual total deposition flux of total mercury ($\mu\text{g m}^{-2} \text{ year}^{-1}$) in India and surrounding regions

typically ranges from 5 to $30 \mu\text{g m}^{-2} \text{ year}^{-1}$ with the highest wet deposition flux of $30 \mu\text{g m}^{-2} \text{ year}^{-1}$ occurring in the northeastern part of the states of Assam and Arunachal Pradesh, a region with extremely high rainfall ranging approximately from 500 to 1000 cm year^{-1} . Other regions that experience a concurrence of relatively high emissions and precipitation also show high wet deposition, including the states of Uttarakhand, Jharkhand, eastern MP and northern Chhattisgarh. Annual wet deposition in southeast Rajasthan is low despite high emissions due to scant rainfall in the arid climate. In general, wet deposition varies by season (not shown here) and is influenced by temporal variability in rainfall.

Huang et al. (2013) measured Hg wet deposition at Lhasa in Tibet. The total annual observed wet deposition over the year 2010, $8.2 \mu\text{g m}^{-2} \text{ year}^{-1}$, was influenced primarily by local industrial sources and human activities. The modeled wet deposition from our study is $5.4 \mu\text{g m}^{-2} \text{ year}^{-1}$. The under-estimate is likely due, in part, to the coarse grid resolution (2° latitude by 2.5° longitude) utilized in the GEOS-Chem model. Use of a finer grid spacing results in better resolution of local source emissions which would result in better spatial resolution of Hg deposition near such sources (e.g., Zhang et al. 2012). The modeled wet deposition over large parts of India ($20\text{--}30 \mu\text{g m}^{-2} \text{ year}^{-1}$) is higher than the range of wet deposition ($2.6\text{--}19.8 \mu\text{g m}^{-2} \text{ year}^{-1}$) measured in North America in 2015 at the Mercury Deposition Network (MDN) stations (NADP 2015). The difference would be larger with a finer

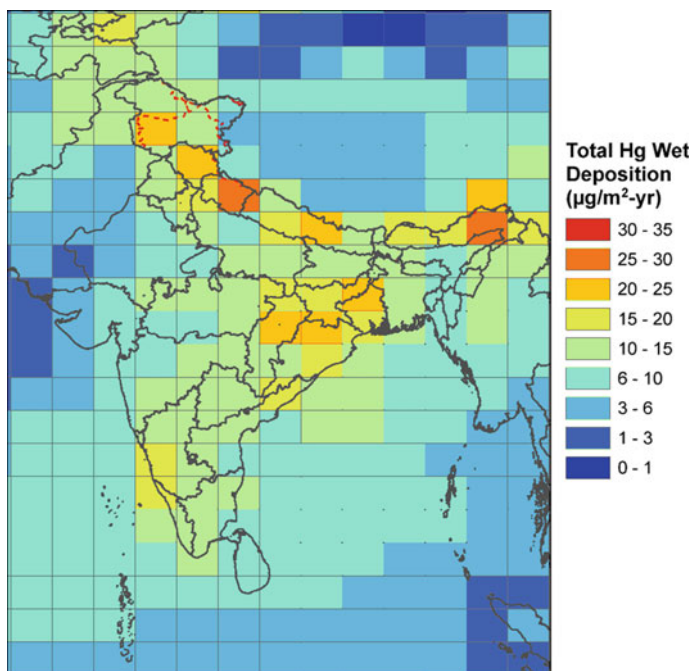


Fig. 13.7 Annual wet deposition flux of total mercury ($\mu\text{g m}^{-2} \text{ year}^{-1}$) in India and surrounding regions

modeling grid and higher modeled wet deposition. The peak modeled Hg wet deposition worldwide is $30 \mu\text{g m}^{-2} \text{ year}^{-1}$ (not shown here). Thus, peak modeled wet deposition in India is comparable to the highest deposition modeled in the world and reflects the confluence of relatively high emissions and high precipitation in India.

The spatial distribution of dry Hg deposition in India (Fig. 13.8) closely reflects the emissions footprint discussed previously (Fig. 13.4).

The maximum annual dry deposition ($35 \mu\text{g m}^{-2} \text{ year}^{-1}$) is predicted in the area spanning northern Chhattisgarh, northern Odisha and southern Jharkhand with a 50% contribution from Hg^{II} , 47% from Hg^{I} , and 3% from Hg_p . The peak modeled dry deposition in India is considerably less than the worldwide maximum of $100 \mu\text{g m}^{-2} \text{ year}^{-1}$. Dry deposition over most of India is also less than the dry deposition modeled in China (typically $25\text{--}75 \mu\text{g m}^{-2} \text{ year}^{-1}$ in this study) reflecting the over fourfold higher Hg emissions in the latter.

Across India on average and at the area of peak total deposition (northern Chhattisgarh), dry deposition is higher by approximately 20% over wet deposition (Table 13.2), with gaseous Hg^{II} dominating wet deposition while dry deposition is dominated by both Hg^{II} and Hg^0 .

There are several sources of uncertainty in these results. A relatively large grid resolution was utilized in this study. Use of a finer grid would better capture the

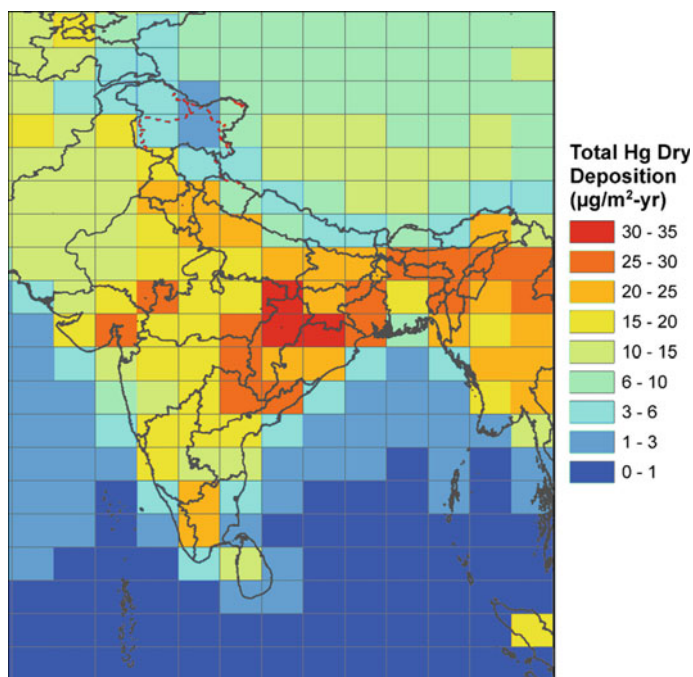


Fig. 13.8 Annual dry deposition flux of total mercury ($\mu\text{g m}^{-2} \text{ year}^{-1}$) in India and surrounding regions

Table 13.2 Speciated annual mercury deposition fluxes in India ($\mu\text{g m}^{-2} \text{ year}^{-1}$)

	Average across India	At location of maximum deposition
Total Hg	27.6	56.3
Dry Hg	15.2	35.0
Wet Hg	12.4	21.3
Hg ⁰ dry	7.9	16.5
Hg ^{II} dry	7.0	17.7
Hg _p dry	0.3	0.8
Hg ^{II} wet	11.0	18.3
Hg _p wet	1.4	3.0

large spatial variability of deposition near sources (Seigneur et al. 2003; Zhang et al. 2012). Future work should apply a regional chemistry transport model with finer grid spacing using boundary conditions from Hg air concentrations simulated by the global modeling system (e.g., Seigneur et al. 2004; Lin et al. 2006; Vijayaraghavan et al. 2007, 2008; Bullock et al. 2008; Zhu et al. 2015). More monitors for mercury wet deposition and air concentrations (e.g., Kumari et al. 2015; Pirrone et al. 2016)

are required in India for model evaluation. This study does not consider litterfall Hg deposition (Wang et al. 2016) nor the small amounts of direct methylmercury deposition from the atmosphere, both of which would increase total predicted deposition amounts. Due to atmospheric transport over very long distances in the free troposphere, the contribution of Hg from sources upwind of India to deposition in India would depend on the accuracy of characterization of those upwind emission sources.

The Government of India promulgated emission standards for Hg emissions for coal-based thermal power plants in December 2015 (<http://pib.nic.in/newsite/PrintRelease.aspx?relid=133726>). Emission control measures adopted to meet these standards would lower the predicted Hg deposition rates across India. However, some of the potential reductions in deposition due to these measures may be offset by growth in coal-based thermal power plants and in production of cement and non-ferrous metals and other anthropogenic sources of mercury across the country.

References

- Amos HM, Jacob DJ, Holmes CD, Fisher JA, Wang Q, Yantosca RM, Corbitt ES, Galarneau E, Rutter AP, Gustin MS, Steffen A, Schauer JJ, Graydon JA, Louis VLS, Talbot RW, Edgerton ES, Zhang Y, Sunderland EM (2012) Gas-particle partitioning of atmospheric Hg(II) and its effect on global mercury deposition. *Atmos Chem Phys* 12:591–603
- AMAP/UNEP (Arctic Monitoring and Assessment Programme/ United Nations Environment Programme) (2013) Technical background report for the global mercury assessment. Arctic monitoring and assessment programme. Oslo, Norway/UNEP Chemicals Branch, Geneva, Switzerland. vi + 263 pp
- AMAP/UNEP (2015) Global mercury modelling: update of modelling results in the global mercury assessment 2013. Arctic monitoring and assessment programme. Oslo, Norway/UNEP Chemicals Branch, Geneva, Switzerland. iv + 32 pp
- Bey I, Jacob DJ, Yantosca RM, Logan JA, Field BD, Fiore AM, Li Q, Liu HY, Mickley LJ, Schultz MG (2001) Global modeling of tropospheric chemistry with assimilated meteorology: Model description and evaluation. *J Geophys Res* 106:23073–23095
- Bullock OR, Atkinson D, Braverman T, Civerolo K, Dastoor A, Davignon D, Ku J, Lohman K, Myers T, Park R, Seigneur C, Selin N, Sistla G, Vijayaraghavan K (2008) The North American Mercury model intercomparison study (NAMMIS): study description and model-to-model comparisons. *J Geophys Res* 113:D17310. <https://doi.org/10.1029/2008JD009803>
- Chakraborty LB, Qureshi A, Vadenbo C, Hellweg S (2013) Anthropogenic mercury flows in India and impacts of emission controls. *Environ Sci Tech* 47(15):8105–8113
- Chen L, Wang HH, Liu JF, Tong YD, Ou LB, Zhang W, Hu D, Chen C, Wang XJ (2014) Intercontinental transport and deposition patterns of atmospheric mercury from anthropogenic emissions. *Atmos Chem Phys* 14:10163–10176. <https://doi.org/10.5194/acp-14-10163-2014>
- Clarkson TW, Magos L, Myers GJ (2003) The toxicology of mercury—current exposures and clinical manifestations. *New Engl J Med* 349:1731–1737. <https://doi.org/10.1056/NEJMra022471>
- Corbitt ES, Jacob DJ, Holmes CD, Streets DG, Sunderland EM (2011) Global source–receptor relationships for mercury deposition under present-day and 2050 emissions scenarios. *Environ Sci Technol* 45:10477–10484

- Driscoll CT, Mason RP, Chan HM, Jacob DJ, Pirrone N (2013) Mercury as a global pollutant: Sources, pathways, and effects. *Environ Sci Technol* 47(4967–4983):2013. <https://doi.org/10.1021/es305071v>
- Giang A, Stokes LC, Streets DG, Corbitt ES, Selin NE (2015) Impacts of the Minamata convention on mercury emissions and global deposition from coal-fired power generation in Asia. *Environ Sci Technol* 49(9):5326–5335
- Guttikunda S, Jawahar P (2014) Atmospheric emissions and pollution from the coal-fired thermal power plants in India. *Atmos Environ* 92:449–460. <https://doi.org/10.1016/j.atmosenv.2014.04.057>
- Holmes CD, Jacob DJ, Corbitt ES, Mao J, Yang X, Talbot R, Slemr F (2010) Global atmospheric model for mercury including oxidation by bromine atoms. *Atmos Chem Phys* 10:12037–12057
- Huang J, Kang SC, Wang SX, Wang L, Zhang QG, Guo JM, Wang K, Zhang GS, Tripathee L (2013) Wet deposition of mercury at Lhasa, the capital city of Tibet. *Sci Total Environ* 447:123–132. <https://doi.org/10.1016/j.scitotenv.2013.01.003>
- Kumari A, Kumar B, Manzoor S, Kulshrestha U (2015) Status of atmospheric mercury research in South Asia: a review. *Aerosol Air Qual Res* 15:1092–1109
- Lindberg S, Bullock R, Ebinghaus R, Engstrom D, Feng X, Fitzgerald W, Pirrone N, Prestbo E, Seigneur C (2007) A synthesis of progress and uncertainties in attributing the sources of mercury in deposition. *Ambio* 36:19–32
- Lin C-J, Pongprueksa P, Lindberg SE, Pehkonen SO, Byun D, Jang C (2006) Scientific uncertainties in atmospheric mercury models I: model science evaluation. *Atmos Environ* 40:2911–2928
- Liu H, Jacob DJ, Bey I, Yantosca RM (2001) Constraints from 210Pb and 7Be on wet deposition and transport in a global three-dimensional chemical tracer model driven by assimilated meteorological fields. *J Geophys Res* 106:12109–12128
- Mukherjee AB, Bhattacharya P, Sarkar A, Zevenhove R (2009) Mercury emissions from industrial sources in India and its effects in the environment (Chapter 4). In: Pirrone N, Mason R (eds) *Mercury fate and transport in the global atmosphere*. Report of the UNEP global partnership on atmospheric mercury transport and fate research, pp 81–112
- National Atmospheric Deposition Program (NADP) (2015) Mercury deposition network (MDN). Champaign. Available from: <http://nadp.isws.illinois.edu/mdn/>
- Pirrone N, Mahaffey KR (2005) Dynamics of mercury pollution on regional and global scales. Atmospheric processes and human exposures around the world. Springer, Berlin
- Pirrone N, Cinnirella S, Feng X, Finkelman RB, Friedli HR, Leaner J, Mason R, Mukherjee AB, Stracher GB, Streets DG, Telmer K. (2010) Global mercury emissions to the atmosphere from anthropogenic and natural sources. *Atmos Chem Phys* 10:5951–30 5964. <https://doi.org/10.5194/acp-10-5951-2010>
- Pirrone N, Sprovieri F, Ebinghaus R (2016) Global mercury observation system—atmosphere (GMOS-A). *Atmos Chem Phys Special Issue* 2016
- Qureshi A, MacLeod M, Hungerbühler K (2011) Quantifying uncertainties in the global mass balance of mercury. *Global Biogeochem Cycles* 25:GB4012
- Qureshi A (2016) Simple box modeling of mercury cycling in the Indian environment. Possible impacts of control scenarios and need for data (preliminary). Presented at the 2016 atmospheric mercury monitoring workshop, Bangkok, Thailand. Available at http://rsm2.atm.ncu.edu.tw/apmmn/PDF/2016/Presentation/21_Simple_box_modeling_of_mercury_cycling_in_the_Indian.pdf. July 27, 2016
- Rai VK, Raman NS, Choudhary SK (2013) Mercury emissions control from coal fired thermal power plants in India: critical review & suggested policy measures. *Int J Eng Res Technol (IJERT)* 2(11)
- Schroeder WH, Munthe J (1998) Atmospheric mercury—an overview. *Atmos Environ* 29:809–822
- Seigneur C, Karamchandani P, Lohman K, Vijayaraghavan K, Shia R-L (2001) Multiscale modeling of the atmospheric fate and transport of mercury. *J Geophys Res* 106:27795–27809
- Seigneur C, Karamchandani P, Vijayaraghavan K, Shia R-L, Levin L (2003) On the effect of spatial resolution on atmospheric mercury modeling. *Sci Total Environ* 304:73–81

- Seigneur C, Vijayaraghavan K, Lohman K, Karamchandani P, Scott C (2004) Global source attribution for mercury deposition in the United States. *Environ Sci Technol* 38:555–569
- Seigneur C, Vijayaraghavan K, Lohman K (2006) Atmospheric mercury chemistry: Sensitivity of global model simulations to chemical reactions. *J Geophys Res* 111:D22306
- Selin NE, Jacob DJ, Park RJ, Yantosca RM, Strode S, Jaeglé L, Jaffe D (2007) Chemical cycling and deposition of atmospheric mercury: global constraints from observations. *J Geophys Res* 112:D02308
- Selin NE, Jacob DJ, Yantosca RM, Strode S, Jaeglé L, Sunderland EM (2008) Global 3-D land-ocean-atmosphere model for mercury: Present-day versus preindustrial cycles and anthropogenic enrichment factors for deposition. *Global Biogeochem Cycles* 22:GB2011
- Sloss L (2012) Mercury emissions from India and South East Asia. ISBN 978-92-9029-528-0. IEA Clean Coal Centre
- Soerensen AL, Sunderland EM, Holmes CD, Jacob DJ, Yantosca RM, Skov H, Christensen JH, Strode SA, Mason RP (2010) An improved global model for air-sea exchange of mercury: high concentrations over the North Atlantic. *Environ Sci Technol* 44:8574–8580
- Song S, Selin NE, Soerensen AL, Angot H, Artz R, Brooks S, Brunke E-G, Conley G, Dommergue A, Ebinghaus R, Holsen TM, Jaffe DA, Kang S, Kelley P, Luke WT, Magand O, Marumoto K, Pfaffhuber KA, Ren X, Sheu G-R, Slemr F, Warneke T, Weigelt A, Weiss-Penzias P, Wip DC, Zhang Q (2015) Top-down constraints on atmospheric mercury emissions and implications for global biogeochemical cycling. *Atmos Chem Phys* 15:7103–7125
- Streets DG, Zhang Q, Wu Y (2009) Projections of global mercury emissions in 2050. *Environ Sci Technol* 43:2983–2988
- Strode SA, Jaeglé L, Selin NE, Jacob DJ, Park RJ, Yantosca RM, Mason RP, Slemr F (2007) Air-sea exchange in the global mercury cycle. *Global Biogeochem Cycles* 21:GB1017
- van der Werf GR, Randerson JT, Giglio L, Collatz GJ, Mu M, Kasibhatla PS, Morton DC, DeFries RS, Jin Y, van Leeuwen TT (2010) Global fire emissions and the contribution of deforestation, savanna, forest, agricultural, and peat fires (1997–2009). *Atmos Chem Phys* 10:11707–11735. <https://doi.org/10.5194/acp-10-11707-2010>
- Vijayaraghavan K, Seigneur C, Karamchandani P, Chen S-Y (2007) Development and application of a multi-pollutant model for atmospheric mercury deposition. *J App Meteorol Climatol* 46:1341–1353
- Vijayaraghavan K, Karamchandani P, Seigneur C, Balmori R, Chen S-Y (2008) Plume-in-grid modeling of atmospheric mercury. *J Geophys Res* 113:D24305. <https://doi.org/10.1029/2008JD010580>
- Vijayaraghavan K, Levin L, Parker L, Yarwood G, Streets D (2014) Response of fish tissue mercury in a freshwater lake to local, regional, and global changes in mercury emissions. *Environ Toxicol Chem* 33:1238–1247
- Wang X, Bao Z, Lin C-J, Yuan W, Feng X (2016) Assessment of global mercury deposition through litterfall. *Environ Sci Technol*. <https://doi.org/10.1021/acs.est.5b06351>
- Wesely ML (1989) Parameterization of surface resistances to gaseous dry deposition in regional-scale numerical models. *Atmos Environ* 23:1293–1304
- Zhang Y, Jaeglé L, van Donkelaar A, Martin RV, Holmes CD, Amos HM, Wang Q, Talbot R, Artz R, Brooks S, Luke W, Holsen TM, Felton D, Miller EK, Perry KD, Schmeltz D, Steffen A, Tordon R, Weiss-Penzias P, Zsolway R (2012) Nested-grid simulation of mercury over North America. *Atmos Chem Phys* 12:6095–6111. <https://doi.org/10.5194/acp-12-6095-2012>
- Zhang Y, Jacob DJ, Horowitz HM, Chen L, Amos HM, Krabbenhoft DP, Slemr F, St. Louis VL, Sunderland EM (2016) Observed decrease in atmospheric mercury explained by global decline in anthropogenic emissions. *Proc Natl Acad Sci (PNAS)* 113(3)
- Zhu J, Wang T, Bieser J, Matthias V (2015) Source attribution and process analysis for atmospheric mercury in eastern China simulated by CMAQ-Hg. *Atmos Chem Phys* 15:8767–8779. <https://doi.org/10.5194/acp-15-8767-2015>